

## ORIGINAL ARTICLE

## Brain sparing in fetal mice: BOLD MRI and Doppler ultrasound show blood redistribution during hypoxia

Lindsay S Cahill<sup>1</sup>, Yu-Qing Zhou<sup>1</sup>, Mike Seed<sup>2,3</sup>, Christopher K Macgowan<sup>2,3,4</sup> and John G Sled<sup>1,4</sup>

Mice reproduce many features of human pregnancy and have been widely used to model disorders of pregnancy. However, it has not been known whether fetal mice reproduce the physiologic response to hypoxia known as brain sparing, where blood flow is redistributed to preserve oxygenation of the brain at the expense of other fetal organs. In the present study, blood oxygen level-dependent (BOLD) magnetic resonance imaging (MRI) and Doppler ultrasound were used to determine the effect of acute hypoxia on the fetal blood flow in healthy, pregnant mice. As the maternal inspired gas mixture was varied between 100% and 8% oxygen on the timescale of minutes, the BOLD signal intensity decreased by  $44 \pm 18\%$  in the fetal liver and by  $12 \pm 7\%$  in the fetal brain. Using Doppler ultrasound measurements, mean cerebral blood velocity was observed to rise by  $15 \pm 8\%$  under hypoxic conditions relative to hyperoxia. These findings are consistent with active regulation of cerebral oxygenation and clearly show brain sparing in fetal mice.

*Journal of Cerebral Blood Flow & Metabolism* (2014) **34**, 1082–1088; doi:10.1038/jcbfm.2014.62; published online 9 April 2014

**Keywords:** BOLD MRI; brain sparing; Doppler ultrasound; fetal mice; hypoxia

## INTRODUCTION

Intrauterine hypoxia is estimated to affect 0.6–0.8% of pregnancies<sup>1</sup> and is correlated with increased risk of perinatal mortality and impaired neurodevelopment.<sup>2,3</sup> Acute fetal hypoxia is often associated with *brain sparing* whereby a greater proportion of oxygenated blood is directed to the brain at the expense of other organs.<sup>4–6</sup> However, in extreme situations, the fetus's capacity for compensation is exceeded and can result in hypoxic-ischemic brain injury.<sup>7</sup> Improvement in outcome for hypoxic fetuses has been reported after continuous maternal oxygen therapy.<sup>8,9</sup> A recent magnetic resonance imaging (MRI) study of healthy human fetuses showed that during exposure to maternal hyperoxia, the oxygenation of several fetal organs increased while oxygenation of the fetal brain remains constant, termed *reversed brain sparing*.<sup>10</sup> Understanding the physiology of this brain sparing response may lead to better diagnostic procedures for predicting fetal risk.

Doppler ultrasound is presently the standard tool for monitoring human fetal well-being. A recent meta-analysis concluded that umbilical artery velocity patterns were moderately useful in predicting fetal distress.<sup>11</sup> Doppler ultrasound measurements at the middle cerebral artery (MCA) have showed brain sparing physiology by detecting reductions in the pulsatility of blood flow in cases of fetal growth restriction<sup>12</sup> and in fetuses with congenital heart disease.<sup>13</sup> Doppler ultrasound measures the velocity of the flowing blood but does not provide direct information on fetal oxygenation. The information provided by ultrasound can be combined with blood oxygen level-dependent (BOLD) MRI, which provides a noninvasive method for measuring the relative state of oxygenation of the fetus and has been shown in both

humans<sup>10,14</sup> and sheep.<sup>15–17</sup> Blood oxygen level-dependent MRI is based on the different magnetic properties of oxyhemoglobin (diamagnetic) and deoxyhemoglobin (paramagnetic) and uses T2\*-weighted imaging to measure changes in the oxygen saturation of blood.<sup>18</sup> An increase in the concentration of deoxyhemoglobin results in a decrease in signal intensity (SI) in BOLD MR images.

The majority of the animal research on pregnancy has been conducted in sheep models.<sup>19</sup> However, the risk of transferring Q fever from sheep to humans has resulted in the removal of sheep from many animal research facilities.<sup>20</sup> Besides considerations of availability, mice offer a number of advantages for modeling complications of pregnancy. Mice reproduce many of the physiologic and molecular features of human pregnancy<sup>21,22</sup> while being efficient for research because of their low cost, rapid gestation, and large litter sizes. Both mice and humans have a hemochorial placenta with a very similar vascular and cellular structure.<sup>21,23,24</sup> Moreover, there are many powerful techniques for genetic manipulation in mice, allowing the generation of mouse models to analyze the mechanisms of placental and fetal development and function.<sup>25</sup> The use of inbred strains leads to genetically identical specimens with reproducible pathology, providing opportunities to test experimental therapies and use a broad range of outcome measures.

In the present study, BOLD MRI and Doppler ultrasound are used to characterize the redistribution of fetal blood flow that occurs in healthy, pregnant mice under hyperoxic and hypoxic conditions. The oxygen content of the gas mixture inhaled by the dam was varied to simulate placental dysfunction. Cycling between maternal hyperoxia and hypoxia will produce the largest

<sup>1</sup>Mouse Imaging Centre, The Hospital for Sick Children, Toronto, Ontario, Canada; <sup>2</sup>Division of Cardiology, Department of Paediatrics, The Hospital for Sick Children, Toronto, Ontario, Canada; <sup>3</sup>Diagnostic Imaging, The Hospital for Sick Children, Toronto, Ontario, Canada and <sup>4</sup>Department of Medical Biophysics, University of Toronto, Toronto, Ontario, Canada. Correspondence: Dr LS Cahill, Mouse Imaging Centre, The Hospital for Sick Children, 25 Orde Street, Toronto, Ontario, Canada M5T 3H7. E-mail: lcahill@mouseimaging.ca

This study was funded by Canadian Institutes of Health Research Grant MOP231389 and the Ontario Research Fund.

Received 29 October 2013; revised 10 March 2014; accepted 17 March 2014; published online 9 April 2014

change in oxygenation of the fetal organs and spans the two conditions where brain sparing is thought to occur. Blood oxygen level-dependent contrast was measured in the fetal brain and fetal liver and Doppler blood velocity was measured in the cerebral arteries.

## MATERIALS AND METHODS

### Animals

A total of 11 healthy adult CD-1 mice from Charles River Laboratories (St Constant, QC, Canada) were used and mated in house (6 for MRI and 5 for ultrasound biomicroscopy). CD-1 mice are an outbred strain often used to study normal pregnancy and fetal development. The morning that a vaginal copulation plug was detected was designated as E0.5. Pregnant mice were imaged at 17.5 days gestation (full term for this strain is 18.5 days). All animal experiments were approved by the Animal Care Committee at the Toronto Centre for Phenogenomics and conducted in accordance with guidelines established by the Canadian Council on Animal Care.

### Hyperoxia and Hypoxia Protocol

Pregnant mice were anesthetized with an intraperitoneal injection of ketamine (150 mg/kg) and xylazine (10 mg/kg). Mice were then endotracheally intubated (22 gauge catheter), placed in a purpose built holder, and mechanically ventilated using a pressure-controlled ventilator (TOPO Small Animal Ventilator; Kent Scientific, Torrington, CT, USA). The oxygen content of the gas mixture inhaled by the dam during the preparation for imaging was 100% O<sub>2</sub>, ensuring the fetal and maternal oxygen saturation was stable at the beginning of the experiment. For one of the dams,

the maternal partial pressure of carbon dioxide was monitored using a transcutaneous blood gas analyzer (TCM4; Radiometer, Cleveland, OH, USA) to verify that normocapnia was maintained throughout the experiment. The same ventilation parameters were used for all of the dams in the study (130 to 150 cycles per minute). Temperature was maintained at 35 to 37°C. The oxygen content of the gas mixture inhaled by the dam was cycled between 100% O<sub>2</sub> (hyperoxia) and 8% O<sub>2</sub> (balance N<sub>2</sub>) (hypoxia) for a total of three cycles. For the ultrasound measurements, the duration of exposure to 8% O<sub>2</sub> for the first, second, and third cycles was 2.8 ± 0.2, 3.3 ± 0.3, and 4.0 ± 1.1 minutes, respectively (mean ± s.d.). For the MRI experiments, the exposure to 8% O<sub>2</sub> was ~4 minutes for each cycle (including scan time and time to manually switch the gas mixtures). To investigate the limits of the brain sparing mechanism, in one of the dams the gas mixture was cycled seven times, resulting in a total exposure time of 50 minutes to 8% O<sub>2</sub>.

### Magnetic Resonance Imaging

Magnetic resonance imaging measurements were performed in six pregnant mice with on average two fetuses examined per dam (Table 1). A 7.0-T, 40-cm horizontal bore magnet (Varian Inc., Palo Alto, CA, USA) equipped with a 29.0-cm inner bore diameter gradient set (Tesla Engineering, Storrington, Sussex, UK) with 120 mT/m maximum amplitude and 870 μs rise time was used to acquire BOLD fetal MR images. A 4-cm inner diameter Millipede RF coil (Varian NMR Systems, Palo Alto, CA, USA) was used to image the whole body. Localizer scans were acquired to find an orientation that corresponded to the mid-sagittal plane of a given fetus. The imaging protocol consisted of a conventional two-dimensional gradient echo sequence with parameters optimized for BOLD contrast at 7.0 T: repetition time = 50 ms, echo time = 10 ms, flip angle = 17°, slice thickness = 1 mm, number of averages = 8, field-of-view = 7.0 × 4.0 mm<sup>2</sup>

**Table 1.** The change in absolute BOLD SI and  $v_{avg}$  with hypoxia for each fetus

Dam	Fetus	Gas condition	Absolute BOLD SI <sup>a</sup>		Change in BOLD SI with hypoxia (%)		$v_{avg}$ (mm/s) <sup>a</sup>	Change in $v_{avg}$ with hypoxia (%) <sup>b</sup>
			Brain	Liver	Brain	Liver		
1	1	100% O <sub>2</sub>	79.9 ± 0.5	52.4 ± 1.1	8 ± 6	69 ± 3		
		8% O <sub>2</sub>	73.5 ± 5.2	16.4 ± 1.6				
	2	100% O <sub>2</sub>	73.5 ± 1.7	18.6 ± 0.5	15 ± 1	36 ± 10		
		8% O <sub>2</sub>	62.4 ± 0.9	11.9 ± 1.9				
2	3	100% O <sub>2</sub>	108.7 ± 0.5	25.2 ± 0.3	16 ± 1	59 ± 8		
		8% O <sub>2</sub>	91.8 ± 1.2	10.2 ± 1.9				
	4	100% O <sub>2</sub>	124.6 ± 1.8	28.7 ± 2.8	14 ± 2	61 ± 4		
		8% O <sub>2</sub>	107.4 ± 1.0	11.2 ± 1.9				
3	5	100% O <sub>2</sub>	118.8 ± 3.5	23.7 ± 1.0	17 ± 6	49 ± 2		
		8% O <sub>2</sub>	99.1 ± 10.1	12.2 ± 1.0				
	6	100% O <sub>2</sub>	105.8 ± 3.5	33.7 ± 2.6	17 ± 13	55 ± 6		
		8% O <sub>2</sub>	87.2 ± 10.8	15.1 ± 0.8				
4	7	100% O <sub>2</sub>	109.0 ± 11.1	20.7 ± 3.3	20 ± 18	20 ± 19		
		8% O <sub>2</sub>	87.0 ± 17.6	16.6 ± 3.3				
5	8	100% O <sub>2</sub>	91.9 ± 2.0	23.3 ± 6.5	8 ± 4	40 ± 12		
		8% O <sub>2</sub>	84.9 ± 2.4	14.0 ± 4.5				
	9	100% O <sub>2</sub>	87.3 ± 1.9	19.0 ± 4.2	8 ± 4	37 ± 6		
		8% O <sub>2</sub>	80.0 ± 2.1	12.1 ± 3.5				
	10	100% O <sub>2</sub>	80.1 ± 3.7	14.6 ± 1.7	6 ± 3	32 ± 17		
		8% O <sub>2</sub>	75.3 ± 1.2	9.7 ± 1.5				
6	11	100% O <sub>2</sub>	108.1 ± 5.5	32.7 ± 14.2	10 ± 6	42 ± 32		
		8% O <sub>2</sub>	97.0 ± 1.8	18.8 ± 2.3				
7	12	100% O <sub>2</sub>					17.4 ± 0.5	22 ± 8
		8% O <sub>2</sub>					22.5 ± 2.0	
8	13	100% O <sub>2</sub>					16.7 ± 0.8	9 ± 1
		8% O <sub>2</sub>					18.2 ± 1.0	
9	14	100% O <sub>2</sub>					11.6 ± 1.5	13 ± 13
		8% O <sub>2</sub>					13.4 ± 0.4	
10	15	100% O <sub>2</sub>					17.0 ± 1.6	14 ± 5
		8% O <sub>2</sub>					19.8 ± 0.6	
11	16	100% O <sub>2</sub>					23.3 ± 0.9	13 ± 6
		8% O <sub>2</sub>					26.8 ± 0.8	

BOLD, blood oxygen level-dependent; MCA, middle cerebral artery; PCA, posterior cerebral artery; SI, signal intensity. <sup>a</sup>Mean ± s.d. over three gas cycles. <sup>b</sup> $v_{avg}$  recorded at either the PCA or the MCA.

and matrix size =  $350 \times 200$ , giving an in-plane resolution of  $200 \mu\text{m}$  and an imaging time of 1.3 minutes per scan. Three images were acquired for each gas condition. Image reconstruction was performed offline using magnitude images.

### Ultrasound Biomicroscopy

Doppler ultrasound measurements were performed in a separate series of pregnant mice (five dams, one fetus/dam) (Table 1). The dams were maintained supine and the hair from the abdomen was removed (using Nair) to improve contact with the transducer. The fetuses were imaged using a high frequency ultrasound system (VisualSonics Vevo 2100, Toronto, ON, Canada) with a 30-MHz linear array transducer.<sup>26,27</sup> Both color flow images and pulsed Doppler velocity spectra for either the posterior cerebral artery (PCA) or MCA were recorded in the fetal mouse at each gas condition. In two dams, the maternal arterial blood oxygen saturation was recorded continuously during the imaging session using an optical pulse oximeter (MouseOx Plus; Starr Life Sciences, Oakmont, PA, USA) placed on the hindlimb.

### Image Analysis

The BOLD SI was determined by defining regions of interest around the entire organ for the fetal brain and fetal liver. Region of interest position was manually adjusted to compensate for minor and infrequent shifts in fetal position (1 to 3 times per imaging session). Motion artifacts were mild and no images were removed from the analysis. For each fetus, the BOLD SI for  $SI_{\text{hypoxia}}$  and  $SI_{\text{hyperoxia}}$  was determined at the final time point of each gas cycle using 8%  $O_2$  (squares in Figure 2D) and 100%  $O_2$  (circles in Figure 2D), respectively. The change in BOLD SI with hypoxia was calculated for each gas cycle as:  $(SI_{\text{hyperoxia}} - SI_{\text{hypoxia}}) / SI_{\text{hyperoxia}}$  and averaged across the three cycles. When multiple fetuses were examined per dam (Table 1), each fetus was treated as a separate measurement.

For the ultrasound measurements, the maximum contour of the Doppler spectrum was traced as a function of time using the Vevo 2100 measurement and analysis software (VisualSonics). The waveforms were summarized in terms of velocity time integral (mm), peak velocity (mm/s), the time averaged maximum velocity ( $v_{\text{avg}}$ , mm/s), pulsatility index (PI), and fetal heart rate.<sup>28</sup> Each parameter was averaged over three cardiac cycles. To compare the increase in cerebral blood flow in different experiments, the time averaged maximum velocity during hypoxic ( $v_{\text{avg(hypoxia)}}$ ) and hyperoxic ( $v_{\text{avg(hyperoxia)}}$ ) conditions was determined by the  $v_{\text{avg}}$  at 2 minutes from the start of each of the gas cycles (before the onset of bradycardia) under 8%  $O_2$  and 100%  $O_2$ , respectively (see Discussion below). The change in  $v_{\text{avg}}$  with hypoxia was calculated for each gas cycle as:  $(v_{\text{avg(hypoxia)}} - v_{\text{avg(hyperoxia)}}) / v_{\text{avg(hypoxia)}}$  and averaged across the three cycles. A similar approach was used to compare the PI during hypoxic and hyperoxic conditions.

### Statistical Analysis

A linear mixed effects model was used to analyze variations in the percent signal change induced by alternating the inspired gas mixture. Total variation was modeled as a sum of interfetal variation and intrafetal variation with the parameters estimated by the reduced maximum likelihood algorithm (lme4 package in R, www.r-project.org). The gas condition was treated as a fixed effect, interfetal variation as a random effect, intrafetal variation as the residual effect, and there were no interaction terms.

## RESULTS

### Qualitative Observations

After the maternal inspired gas mixture was changed from 100%  $O_2$  (hyperoxia) to 8%  $O_2$  (hypoxia), the maternal arterial blood oxygen saturation ( $SpO_2$ ) began to decrease (Figure 1A). The blood flow and  $SpO_2$  did not have time to stabilize at a minimum value during the 3-minute interval of 8%  $O_2$ . The maternal heart rate rose, consistent with acute hypoxia (Figure 1B). Simultaneous measurements from Doppler ultrasound show that the fetal heart rate only decreased slightly until the onset of bradycardia occurred at  $\sim 2.5$  to 3 minutes under 8%  $O_2$  (*vide infra*, Figure 4H). The decrease in fetal heart rate corresponds to a decrease in mean cerebral blood velocity (Figure 4G).

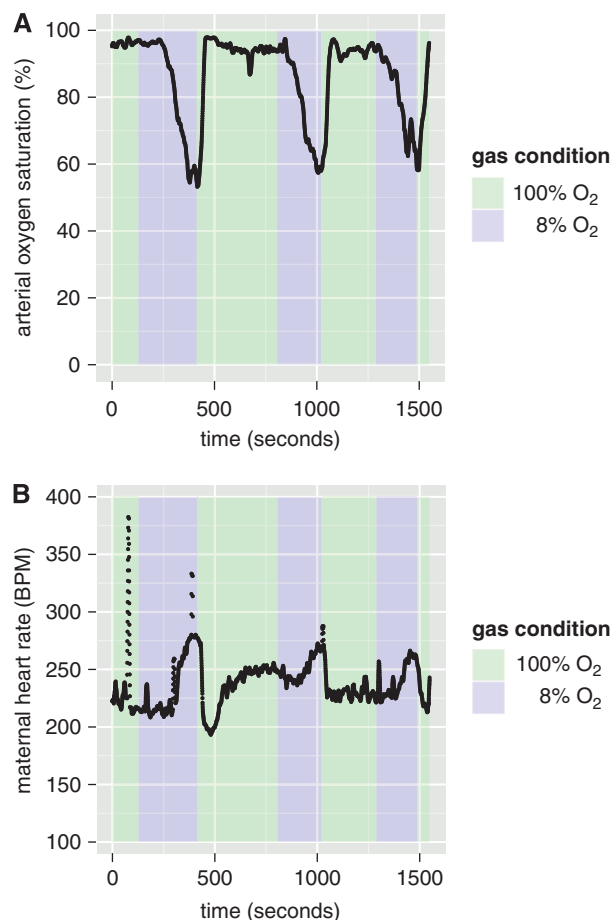


**Figure 1.** Maternal physiologic changes under repeated exposure to acute hypoxia. Scatter plots showing the time course of (A) maternal arterial blood oxygen saturation (%) and (B) maternal heart rate (beats per minute, BPM) as the inspired oxygen mixture is varied. The spikes in the maternal heart rate at 76 and 387 seconds are attributed to instrument noise.

### Quantitative Analyses

The boundaries of the fetal organs are readily identified *in vivo* on a conventional  $T2^*$ -weighted MRI scan. A representative anatomic MRI coronal slice through the abdomen of a pregnant mouse at 17.5 days gestation is shown in Figure 2A. With an in-plane resolution of  $200 \mu\text{m}$ , major fetal anatomic structures including brain, spine, heart, lung, and liver can be identified. Moreover, the tissue contrast is sufficient to allow delineation of these structures (Figures 2B and 2C). The large litter size (typically 10 to 14 in CD-1 mice) and the late gestation period resulted in minimal fetal movement throughout the MRI session. Moreover, maternal respiratory gating was not required, most likely because the fetuses selected for imaging were located at a significant distance from the maternal lungs.

As the maternal inspired gas mixture was varied from 100% to 8%  $O_2$ , a large decrease in the BOLD SI was observed in the fetal liver but not in the fetal brain (Figure 2D). Over the time course of the experiment, the change in the brain and liver SI was reproducible both between repeated measurement trials and across measurement trials. For the brain, the intrafetal standard deviation was 7% and the interfetal effect accounted for an additional 3% of variation. For the liver, the intrafetal and interfetal standard deviations were 14% and 13%, respectively. In the animals studied ( $n = 6$ ), the BOLD SI under hypoxic conditions

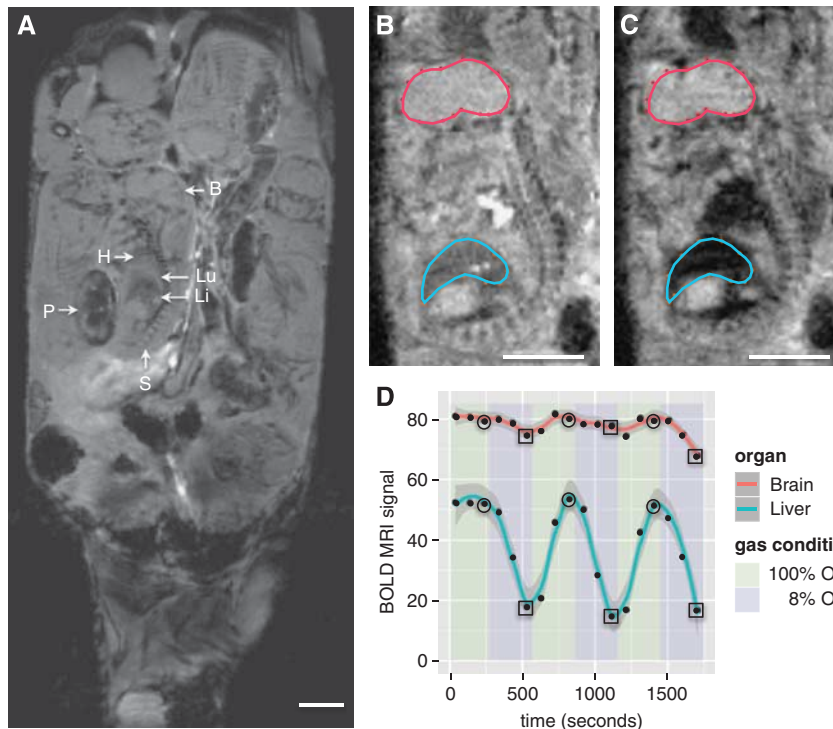


**Figure 2.** Fetal mouse blood oxygen level-dependent contrast magnetic resonance imaging (MRI) signal variation with maternal inspired oxygen. **(A)** Representative coronal anatomic MR image of a 17.5-day gestation dam. Multiple fetuses and placentas are seen in this view. B: brain; H: heart; Li: liver; Lu: lung; P: placenta; S: spine. **(B)** Representative blood oxygen level-dependent (BOLD) MR image of a fetus showing the placement of regions of interest (ROIs) when the dam is breathing 100% O<sub>2</sub> and **(C)** 8% O<sub>2</sub>. The decrease in signal intensity (SI) in the liver during hypoxia is clearly visible. **(D)** Scatter plot showing the absolute BOLD MR signal (arbitrary units) in one of the six dams **(B, C)** as the inspired oxygen mixture is varied. The smoothing (solid red and blue lines) was performed using LOWESS, a robust locally weighted smoothing algorithm.<sup>40</sup>  $SI_{\text{hypoxia}}$  and  $SI_{\text{hyperoxia}}$  were determined by calculating the mean of the SI at the final time point of each gas cycle under 8% O<sub>2</sub> (squares) and 100% O<sub>2</sub> (circles), respectively. Scale bars in **(A)**, **(B)**, and **(C)** = 5 mm.

decreased by  $44 \pm 18\%$  in the liver and by  $12 \pm 7\%$  in the brain. During the 3-minute interval of 8% O<sub>2</sub>, the liver SI did not stabilize at a minimum value, consistent with the continued change in maternal SpO<sub>2</sub> (Figure 1A). To examine the limits of the brain sparing mechanism, we performed repeated cycling of the gas mixtures and prolonged exposure using 8% O<sub>2</sub> ( $n = 1$ ). After 40 minutes of total exposure to 8% O<sub>2</sub>, the BOLD SI decreased by 69% in the brain and by 67% in the liver (Figure 3).

Magnetic resonance images were complemented by ultrasound B-mode and color Doppler images of E17.5 fetuses (Figure 4). Cerebral blood flow, measured by the PCA and MCA blood velocity waveforms, was observed to rise under maternal hypoxic conditions (Figures 4E to 4G). In all of the animals studied ( $n = 5$ ), the normalized  $v_{\text{avg}}$  in the brain under hypoxic conditions increased by  $15 \pm 8\%$ . This measurement was found to be reproducible both between repeated measurement trials and across measurement trials (the intrafetal and interfetal standard deviations were 9% and 0.5%, respectively, for the percent increase in velocity). The mean PI across mice was  $5 \pm 1$  under both hyperoxia and hypoxia and therefore did not change significantly between gas conditions.

## DISCUSSION

In the present study, BOLD contrast MRI and Doppler ultrasound were used to study the redistribution of fetal blood that results from acute maternal and fetal hypoxia. The small BOLD signal change in the brain and the increase in cerebral blood flow under

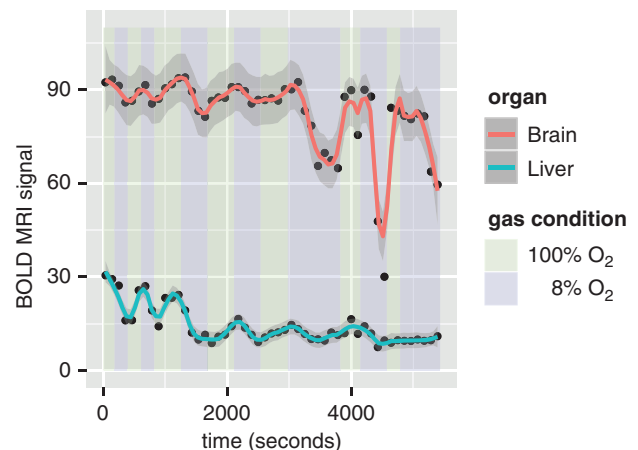


**Figure 3.** Fetal mouse blood oxygen level-dependent contrast magnetic resonance imaging (MRI) signal variation with prolonged hypoxic challenge shows the limits of the brain sparing mechanism. Scatter plot showing the absolute blood oxygen level-dependent (BOLD) MR signal (arbitrary units) in one of the six dams as the inspired oxygen mixture is varied. The smoothing (solid red and blue lines) was performed using LOWESS.

hypoxic conditions are consistent with active regulation of cerebral oxygenation at the expense of other organs, the brain sparing effect. This phenomenon is believed to help preserve the



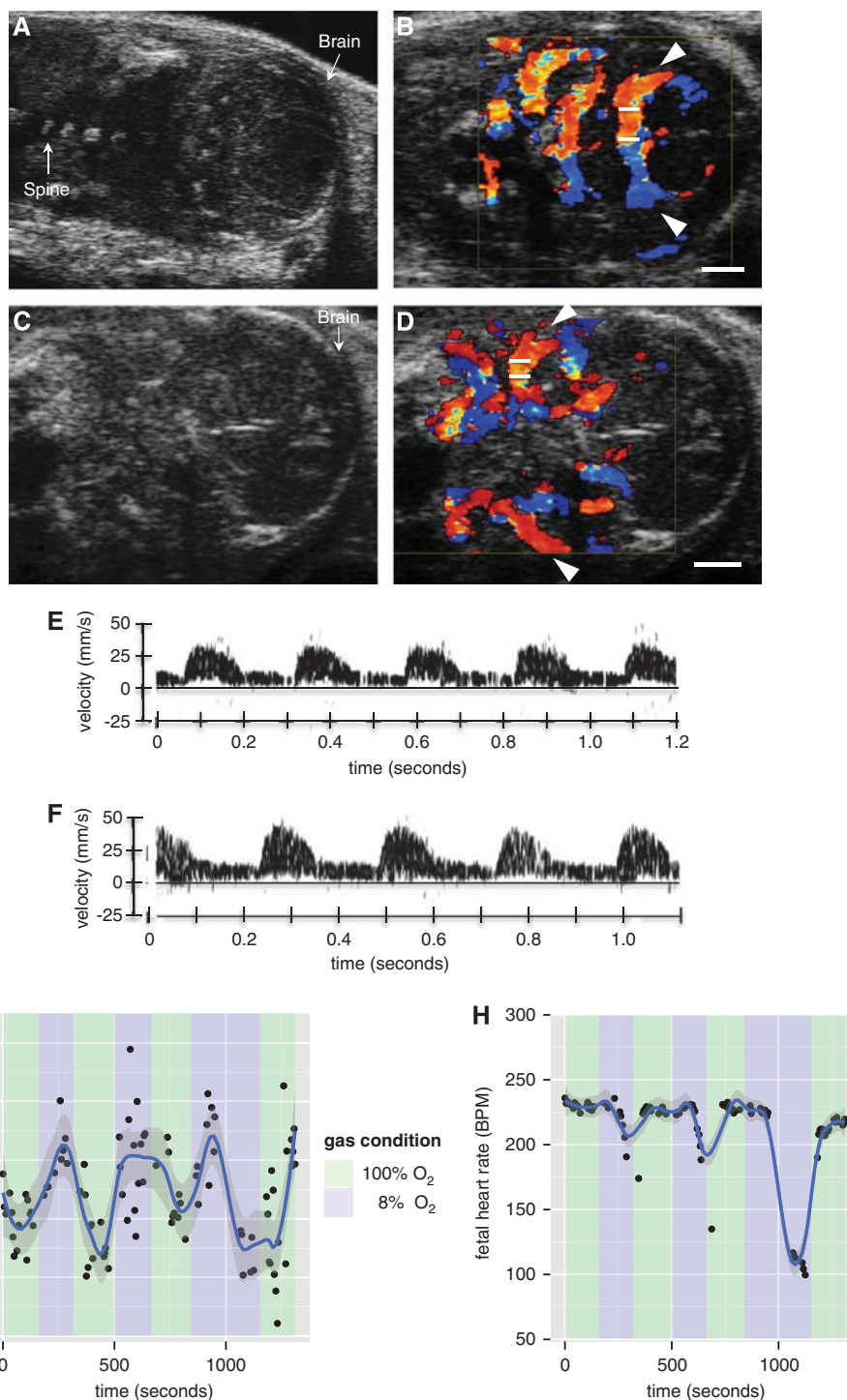


**Figure 4.** Assessment of mouse fetal blood flow by ultrasound biomicroscopy. (**A**, **C**) Representative B-mode images of E17.5 fetuses in coronal section showing the fetal brain. Color Doppler overlay indicating flow direction (red is blood flowing toward the transducer and blue is blood flowing away from the transducer) for the (**B**) posterior cerebral arteries (PCAs) (arrows shown) and (**D**) middle cerebral arteries (MCAs) (arrows shown). The angle of insonation was  $0^\circ$  and  $5^\circ$  for (**B**) and (**D**), respectively. Measurements were taken from the vessel in the near field with the transducer located above the structure in (**B**) and (**D**). The white bars on the vessel of interest represent the location of the Doppler sample volume. (**E**) Doppler blood velocity spectrum versus time for the PCA when the dam is breathing 100%  $O_2$  and (**F**) 8%  $O_2$ . Similar waveforms were recorded for the MCA. (**G**) Scatter plot showing the mean PCA blood flow as the inspired oxygen mixture is varied. (**H**) Scatter plot showing the fetal heart rate (beats per minute, BPM) as the inspired oxygen mixture is varied. The smoothing (blue line) was performed using LOWESS. Scale bars in (**B**) and (**D**) = 1 mm.

supply of oxygen to the fetal brain and other organs that are critical for survival. The BOLD MRI findings are consistent with previous studies during acute hypoxia in fetal sheep<sup>15–17</sup> and the

rise in cerebral blood flow is known to occur in human cases of fetal growth restriction.<sup>29</sup> To our knowledge, this is the first study to show brain sparing in fetal mice.

A striking feature of using the fetal mouse in this manner to study fetal circulatory physiology is the reproducibility of the response both between repeated measurement trials and across measurement trials. In the longest session, we cycled the gas mixture seven times. There are a number of time constants that determined the dynamics of this system. While the dead volume of the gas lines exchanges rapidly, on the order of a few seconds, the maternal oxygen saturation changes over the course of minutes and does not reach its asymptotic value within the 3-minute intervals of hypoxia examined here. On this timescale of minutes, the fetal blood response appears to track the maternal oxygen saturation and these two measures were found to correlate when measured simultaneously ( $R^2=0.476$ , slope =  $-0.07$ ,  $P<0.001$ ). Approximately 1.5 to 2 minutes into the hypoxia interval, with the saturation decreasing below 80%, the maternal heart rate begins to rise, perhaps in part compensating for the decreasing oxygen transport across the placenta. At  $\sim 2.5$  to 3 minutes into the hypoxia interval, with the maternal saturation decreasing below 65%, the fetal heart rate decreases and fetal MCA velocity decreases (see for instance the third 8% O<sub>2</sub> interval in Figures 4G and 4H). We interpret this threshold of 65% maternal oxygen saturation as the point beyond which the fetus decompensates. This threshold does not appear to represent cardiac failure, as the original heart rate returns when maternal oxygen saturation rises and the cycle of compensation and then decompensation is repeated. The decrease in fetal heart rate may explain the large decrease in the BOLD MRI signal in the fetal brain after prolonged exposure to hypoxia (Figure 3). Bradycardia is known to occur in human fetuses during hypoxic conditions,<sup>30</sup> is thought to be mediated by a vagal nerve response<sup>31</sup> and may be the result of the known decrease in oxygen consumption that occurs with severe hypoxia.<sup>32</sup> Our data highlight the importance of fetal heart rate monitoring as a measure of fetal well-being.

The reduction in the BOLD SI in the liver during hypoxia is consistent with the current understanding of fetal circulatory adaptation.<sup>4,31,33,34</sup> The two main sources of blood to the liver are the umbilical vein and the portal vein. During hypoxic conditions, increased blood supply to the brain is achieved by preferential streaming of umbilical venous blood across the ductus venosus, bypassing the liver. Therefore, overall liver perfusion is reduced and the liver is perfused mainly by the less-well-oxygenated portal vein.

The argument that the fetal measurements represent brain sparing is predicated on BOLD providing a measure of tissue oxygenation. This interpretation is supported by sheep data where fetal oxygenation was assessed both by an implanted optode<sup>17</sup> and by fetal arterial blood sampling.<sup>16</sup> Deoxyhemoglobin, which is paramagnetic and by virtue of the complex geometry of the vascular system nonuniformly distributed within the tissue, leads to heterogeneity in the local magnetic field within an organ.<sup>18,35</sup> The more heterogeneous the field strength becomes, the lower is the observed BOLD signal. Hence, the BOLD signal depends both on the geometry of the vascular space and on the deoxyhemoglobin concentration within the blood.<sup>36,37</sup> The BOLD signal also depends on parameters such as local changes in magnetic field, position in the radiofrequency coil and magnetic field shimming. Therefore, the absolute BOLD signal will vary across subjects and across scanning sessions and only relative values of oxygenation can be compared.

Large changes in BOLD were observed in the fetal brain given sufficiently hypoxic conditions. Specifically, we observed a 69% decrease in fetal brain BOLD signal after prolonged exposure to 8% O<sub>2</sub> and a 67% decrease in fetal liver signal. In this context, we interpret as brain sparing the 12% decrease in brain and a 44% decrease in liver BOLD signal observed in conjunction with elevated cerebral blood flow after 2 minutes of hypoxia. In humans, it is believed that fetal cerebral vasodilation, detected as a reduction in pulsatility of blood flow in the MCA, occurs to

maintain oxygen delivery during hypoxia.<sup>13,38</sup> It is unclear that this mechanism of blood redistribution is active in the mouse, as we did not observe a significant change in the PI of the cerebral arteries during hypoxia. This finding may also be due to a difference in vessel composition affecting the propagation and reflection of pressure waves, as mice do not have large elastic vessels. The PI was also found to correlate poorly with vascular resistance in studies of fetal sheep.<sup>39</sup> Understanding the redistribution of blood flow throughout the entire fetal circulation in the mouse during hypoxia is a subject for future investigation.

A limitation of the present study is that the experimental conditions simulate an acute hyperoxic/hypoxic challenge and not a chronic condition such as therapeutic hyperoxia or fetal asphyxia. Moreover, 8% O<sub>2</sub> is too severe a hypoxic challenge for a prolonged experiment as the animal physiology does not reach a steady state and eventually results in fetal decompensation. This limited the Doppler ultrasound measurement of blood flow changes during hypoxia to one organ within each fetus. Future studies, using a less severe hypoxic challenge, will also include measurements of blood velocity in the fetal liver. These acute conditions are nonetheless useful to explore the limits of the model system.

The study of the fetal response to hypoxic conditions is valuable for developing accurate diagnostic procedures for fetal intensive-care monitoring *in utero*. Experimental animals allow us to create highly controlled and reproducible pathology against which we can evaluate our understanding of fetal physiology. Moreover, a broad set of outcome measures can be used in animal studies that test novel interventions. Here, we show that brain sparing physiology is present in the fetal mouse. Combined with murine genetic models of placental insufficiency and impaired metabolism, this observation creates new opportunities to understand the mechanisms of fetal distress and illustrates the value of BOLD MRI as a noninvasive tool to study cerebral autoregulation in the mouse.

## DISCLOSURE/CONFLICT OF INTEREST

The authors declare no conflict of interest.

## ACKNOWLEDGMENTS

The authors thank Dr Monique Rennie for helpful discussions.

## REFERENCES

- 1 Arraut AM, Frias AE, Hobbs TR, McEvoy C, Spindel ER, Rasanen J. Fetal pulmonary arterial vascular impedance reflects changes in fetal oxygenation at near-term gestation in a nonhuman primate model. *Reprod Sci* 2013; **20**: 33–38.
- 2 Hill A. Current concepts of hypoxic-ischemic cerebral injury in the term newborn. *Pediatr Neurol* 1991; **7**: 317–325.
- 3 Lou HC. Perinatal hypoxic-ischemic brain damage and intraventricular hemorrhage. A pathogenetic model. *Arch Neurol* 1980; **37**: 585–587.
- 4 Cohn HE, Sacks EJ, Heymann MA, Rudolph AM. Cardiovascular responses to hypoxemia and acidemia in fetal lambs. *Am J Obstet Gynecol* 1974; **120**: 817–824.
- 5 Gleason CA, Hamm C, Jones Jr. MD. Effect of acute hypoxemia on brain blood flow and oxygen metabolism in immature fetal sheep. *Am J Physiol* 1990; **258**: H1064–H1069.
- 6 Pearce W. Hypoxic regulation of the fetal cerebral circulation. *J Appl Physiol* 2006; **100**: 731–738.
- 7 Jensen A, Garnier Y, Berger R. Dynamics of fetal circulatory responses to hypoxia and asphyxia. *Eur J Obstet Gynecol Reprod Biol* 1999; **84**: 155–172.
- 8 Nicolaidis KH, Campbell S, Bradley RJ, Bilardo CM, Soothill PW, Gibb D. Maternal oxygen therapy for intrauterine growth retardation. *Lancet* 1987; **1**: 942–945.
- 9 Say L, Gulmezoglu AM, Hofmeyr GJ. Maternal oxygen administration for suspected impaired fetal growth. *Cochrane Database Syst Rev* 2003 CD000137.
- 10 Sorensen A, Peters D, Simonsen C, Pedersen M, Stausbol-Gron B, Christiansen OB *et al*. Changes in human fetal oxygenation during maternal hyperoxia as estimated by BOLD MRI. *Prenat Diagn* 2013; **33**: 141–145.

- 11 Morris RK, Malin G, Robson SC, Kleijnen J, Zamora J, Khan KS. Fetal umbilical artery Doppler to predict compromise of fetal/neonatal wellbeing in a high-risk population: systematic review and bivariate meta-analysis. *Ultrasound Obstet Gynecol* 2011; **37**: 135–142.
- 12 Baschat AA. Neurodevelopment following fetal growth restriction and its relationship with antepartum parameters of placental dysfunction. *Ultrasound Obstet Gynecol* 2011; **37**: 501–514.
- 13 Donofrio MT, Bremer YA, Schieken RM, Gennings C, Morton LD, Eidem B *et al*. Autoregulation of cerebral blood flow in fetuses with congenital heart disease: the brain sparing effect. *Pediatr Cardiol* 2003; **24**: 436–443.
- 14 Semple SI, Wallis F, Haggarty P, Abramovich D, Ross JA, Redpath TW *et al*. The measurement of fetal liver T\*(2) in utero before and after maternal oxygen breathing: progress towards a non-invasive measurement of fetal oxygenation and placental function. *Magn Reson Imaging* 2001; **19**: 921–928.
- 15 Wedegartner U, Tchirikov M, Schafer S, Priest AN, Walther M, Adam G *et al*. Fetal sheep brains: findings at functional blood oxygen level-dependent 3-T MR imaging—relationship to maternal oxygen saturation during hypoxia. *Radiology* 2005; **237**: 919–926.
- 16 Wedegartner U, Tchirikov M, Schafer S, Priest AN, Kooijman H, Adam G *et al*. Functional MR imaging: comparison of BOLD signal intensity changes in fetal organs with fetal and maternal oxyhemoglobin saturation during hypoxia in sheep. *Radiology* 2006; **238**: 872–880.
- 17 Sorensen A, Pedersen M, Tietze A, Ottosen L, Duus L, Ulbjerg N. BOLD MRI in sheep fetuses: a non-invasive method for measuring changes in tissue oxygenation. *Ultrasound Obstet Gynecol* 2009; **34**: 687–692.
- 18 Ogawa S, Lee TM, Kay AR, Tank DW. Brain magnetic resonance imaging with contrast dependent on blood oxygenation. *Proc Natl Acad Sci USA* 1990; **87**: 9868–9872.
- 19 Barry JS, Anthony RV. The pregnant sheep as a model for human pregnancy. *Theriogenology* 2008; **69**: 55–67.
- 20 Simor AE, Brunton JL, Salit IE, Vellend H, Ford-Jones L, Spence LP. Q fever: hazard from sheep used in research. *Can Med Assoc J* 1984; **130**: 1013–1016.
- 21 Georgiades P, Ferguson-Smith AC, Burton GJ. Comparative developmental anatomy of the murine and human definitive placentae. *Placenta* 2002; **23**: 3–19.
- 22 Cox B, Kotlyar M, Evangelou AI, Ignatchenko V, Ignatchenko A, Whiteley K *et al*. Comparative systems biology of human and mouse as a tool to guide the modeling of human placental pathology. *Mol Syst Biol* 2009; **5**: 279.
- 23 Adamson SL, Lu Y, Whiteley KJ, Holmyard D, Hemberger M, Pfarrer C *et al*. Interactions between trophoblast cells and the maternal and fetal circulation in the mouse placenta. *Dev Biol* 2002; **250**: 358–373.
- 24 Cross JC, Hemberger M, Lu Y, Nozaki T, Whiteley K, Masutani M *et al*. Trophoblast functions, angiogenesis and remodeling of the maternal vasculature in the placenta. *Mol Cell Endocrinol* 2002; **187**: 207–212.
- 25 Rossant J, Cross JC. Placental development: lessons from mouse mutants. *Nat Rev Genet* 2001; **2**: 538–548.
- 26 Foster FS, Zhang MY, Zhou YQ, Liu G, Mehi J, Cherin E *et al*. A new ultrasound instrument for in vivo microimaging of mice. *Ultrasound Med Biol* 2002; **28**: 1165–1172.
- 27 Zhou YQ, Foster FS, Qu DW, Zhang M, Harasiewicz KA, Adamson SL. Applications for multifrequency ultrasound biomicroscopy in mice from implantation to adulthood. *Physiol Genomics* 2002; **10**: 113–126.
- 28 Phoon CK, Turnbull DH. Ultrasound biomicroscopy-Doppler in mouse cardiovascular development. *Physiol Genomics* 2003; **14**: 3–15.
- 29 Hecher K, Campbell S, Doyle P, Harrington K, Nicolaides K. Assessment of fetal compromise by Doppler ultrasound investigation of the fetal circulation. Arterial, intracardiac, and venous blood flow velocity studies. *Circulation* 1995; **91**: 129–138.
- 30 Hanson MA. Do we now understand the control of the fetal circulation? *Eur J Obstet Gynecol Reprod Biol* 1997; **75**: 55–61.
- 31 Rudolph AM. *Congenital Diseases of the Heart: Clinical-Physiological Considerations*. Wiley-Blackwell: Chichester, 2009.
- 32 Rurak DW, Richardson BS, Patrick JE, Carmichael L, Homan J. Oxygen consumption in the fetal lamb during sustained hypoxemia with progressive acidemia. *Am J Physiol* 1990; **258**: R1108–R1115.
- 33 Kiserud T. Physiology of the fetal circulation. *Semin Fetal Neonatal Med* 2005; **10**: 493–503.
- 34 Sorensen A, Holm D, Pedersen M, Tietze A, Stausbol-Gron B, Duus L *et al*. Left-right difference in fetal liver oxygenation during hypoxia estimated by BOLD MRI in a fetal sheep model. *Ultrasound Obstet Gynecol* 2011; **38**: 665–672.
- 35 Brown GG, Perthen JE, Liu TT, Buxton RB. A primer on functional magnetic resonance imaging. *Neuropsychol Rev* 2007; **17**: 107–125.
- 36 Ogawa S, Menon RS, Kim SG, Ugurbil K. On the characteristics of functional magnetic resonance imaging of the brain. *Annu Rev Biophys Biomol Struct* 1998; **27**: 447–474.
- 37 van Zijl PC, Eleff SM, Ulatowski JA, Oja JM, Ulug AM, Traustman RJ *et al*. Quantitative assessment of blood flow, blood volume and blood oxygenation effects in functional magnetic resonance imaging. *Nat Med* 1998; **4**: 159–167.
- 38 Daven JR, Milstein JM, Guthrie RD. Cerebral vascular resistance in premature infants. *Am J Dis Child* 1983; **137**: 328–331.
- 39 Adamson SL, Langille BL. Factors determining aortic and umbilical blood flow pulsatility in fetal sheep. *Ultrasound Med Biol* 1992; **18**: 255–266.
- 40 Cleveland WS. LOWESS: A program for smoothing scatterplots by robust locally weighted regression. *Am. Stat* 1981; **35**: 54.



This work is licensed under a Creative Commons Attribution-NonCommercial-ShareAlike 3.0 Unported License. To view a copy of this license, visit <http://creativecommons.org/licenses/by-nc-sa/3.0/>